PERFORMANCE OF LITHIUM-POLYMER CELLS AT HIGH HYDROSTATIC PRESSURE

K. Rutherford[*a], D. Doerffel[a]

[a]*School of Engineering Sciences, University of Southampton, Highfield, Southampton, SO17 1BJ, UK*

Abstract

Lithium polymer cells are an attractive energy source for underwater vehicles due to their high specific energy and possible operation at hydrostatic pressure. Their behaviour at pressures experienced in the deep ocean is of particular concern to designers. This paper presents test results that show how the voltage during discharge is affected by temperatures between 4°C and 28°C, and pressures of 0.1 MPa and 60 MPa. A simple non-linear equivalent circuit to model the internal resistance of the cell is shown and the effect of temperature on resistance is found. The main conclusions are that lithium polymer cells can operate at 60 MPa, and their performance is similar to that at 0.1 Mpa. Underwater cold temperature and high current reduce the performance of the cell more than high pressure.

Keywords: Lithium polymer batteries, AUV, high pressure, equivalent circuit.

* Corresponding author. Tel: +44 (0)2380-596004 Fax: +44 (0)2380-596149; E-mail address: K.Rutherford@soton.ac.uk

Nomenclature

C_{12}	Double layer capacitance	F
C_{long}	Diffusion capacitance	F
I_C	Charge current	A
I_D	Discharge current	A
Q_0	Rated capacity of a cell at full charge	Ah
R_{01}	Total ohmic resistance	Ω
R_{12}	Charge transfer resistance on discharge	Ω
R_{Long}	Diffusion resistance	Ω
R_P	Self discharge resistance	Ω
S_B	Battery specific energy	Wh kg^{-1}
SOC	State of charge	%
S_S	System specific energy	Wh kg^{-1}
V_0	Voltage at beginning of pause in discharge	V
V_1	Voltage at the end of instantaneous voltage rise	V
V_2	Voltage after 900 seconds of pause.	V

1. Introduction

The motivation for this study was to investigate a potential power source for use within battery-powered autonomous underwater vehicles (AUVs), in particular AUVs that dive deep, to over 5000 m. The Southampton Oceanography Centre's Autosub AUV has operated with batteries assembled from manganese alkaline 'D' size primary cells since 1998, completing over 300 missions for marine science [1]. In the current design, the batteries, made up from up to 5000 cells, are housed in four carbon fibre reinforced plastic tubes, rated to an operating depth of 1600 m [2]. The longest mission to date has been 253 km, limited by the energy that was available [3]. As reliability of the vehicles' systems has improved over the last six years the mission endurance becomes limited by the energy available on board rather than by system failures. AUVs are subject to the limitations of terrestrial electric vehicles, but have additional constraints, such as the need to design for near neutral buoyancy, while providing sufficient energy for missions. Autosub requires over 150 MJ for a 250 Km mission, with typically 500 W in propulsion and 500 W in control system and sensors. In turn, choice of power source affects the mass, shape, performance, and cost of operation of the vehicle.

To date, most AUVs use batteries as their power source. These batteries are usually enclosed within pressure vessels, providing dry space at one atmosphere pressure. However, Stevenson and Graham [4] show that the mass to displacement ratio of pressure vessels increases with diving depth. There is an increasing mass penalty in providing space at one atmosphere for the energy system as a whole (batteries and pressure vessel) for deep diving vehicles.

As a consequence, especially for deep diving vehicles, the option to remove the need for the pressure vessels by operating the batteries at ambient pressure would prove highly advantageous [5]. The batteries would displace their own volume of water, reducing the mass of buoyancy required to float the battery system.

However, not all cell chemistries or forms of construction are amenable to operation at ambient pressures of up to 60 MPa (6000 m water depth). Pressure compensated lead-acid cells are in routine use within instruments and vehicles used in the deep sea, for example the valve-regulated Seabattery [6]. However, their specific energy is low (e.g. 21 Wh kg^{-1} for the 12V 48Ah Seabattery). One candidate cell chemistry with a high specific energy and a form of construction expected to be tolerant to pressure is the lithium-polymer cell (e.g.194 Wh Kg^{-1} for the Kokam SLPB526495 [7]).

As yet, there appears to be no open-literature papers on the performance of lithium-polymer cells at high pressure.

This paper reports the results of experiments to evaluate the electrical and mechanical performance of one type of lithium-polymer pouch cells (Kokam SLPB526495 cells rated at 3.27 Ah [7]) under hydrostatic pressure, with a view towards their use in a new deep-diving AUV Autosub-6000.

Cells were first tested at atmospheric pressure and at ambient temperature. This established typical cell capacity and discharge performance, and provided the parameters of a simple equivalent circuit model used previously for lithium-ion cells by AbuSharkh and Doerffel [8]. Furthermore this data provided a reference to compare the performance and characteristics of cells tested at high pressure (60 MPa) or at low temperature (4˚C), typical of the deep ocean. Due to practical constraints it was not possible to alter the temperature of the pressure vessel, preventing the determination of cell performance at the combination of low temperature and high pressure.

2. Methods.

2.1 Test procedures

The experiments under pressure were made within a water-filled cylindrical pressure vessel. The cell was placed within deformable bags filled with oil to ensure electrical insulation and isobaric pressure. The cell was tested with a Digatron universal battery tester as described by Doerffel and Abu Sharkh [8]. The temperature was measured with a thermistor attached to the cell terminal. The same cell was used for the atmospheric pressure tests at 18°C and the tests at 60MPa. A separate cell had to be wired up to test the differing temperature effects.

For reasons of safety, the initial survival test pressurised one cell only to 60 MPa for 1 hour. On depressurisation, the cell was inspected for signs of damage and its terminal and on load voltages checked. These tests showed that this type of lithium-polymer cells would be able to survive the test procedure physically and electrically. Further tests where conducted where batches of 50 cells were pressurised for a total of 12 cycles and then tested electrically, zero failures gave additional confidence that the cells would be suitable for use in pressure compensated batteries.

The electrical test cycle consisted of a full charge with a current of 1 A, until the terminal voltage reached 4.2 V. Charging then continued at this voltage until the current fell below 0.327 A. At this point the cell was considered to be fully charged (100%) SOC. During charging, pauses for 15 minutes were inserted after each 0.327 Ah of charge, representing 10% SOC increase.

During discharge the current was held at a constant value. The cell was considered to be discharged when the on-load voltage reached 3V, above the absolute minimum of 2.5 V as recommended by manufacturer [7]. During discharge pauses of 15 minutes at 0.327Ah intervals meant the peaks in the voltage recovery would align, easing the calculation of OCV using the procedure suggested in [8]. The cell was allowed to rest for 2 hours after a discharge, or at least 4 hours after a charge, to allow the cell to reach close to equilibrium state

One cell, chosen as reference, underwent electrical cycles at 26°C and atmospheric pressure to establish baseline charge discharge characteristics and capacity (section 3.1). Further tests varied the temperature of the air surrounding the cell and the current drawn during discharge at

atmospheric pressure (section 3.1) and at 60 MPa (section 3.2)

A simple method was used to calculate state of charge (SOC), which assumes each cell was fully charged before the start of each test, and that subsequent cycles charged to the same point. Q_o is assumed to be the nominal cell capacity of 3.27 Ah.

$$SOC(t) = 100\frac{Q_o - \int_0^t I_D(t)dt}{Q_o} \quad (1)$$

2.2 Derivation of the equivalent circuit parameters

As well as determining any effect of hydrostatic pressure on capacity, experiments sought to identify any changes in the internal resistance of the cell. The equivalent circuit of the cell is modelled as a simple linear passive network (Fig. 1) based on a Randles configuration. As this representation does not account for complex nonlinearities, the circuit parameters are functions of temperature, current, state of charge and perhaps pressure.

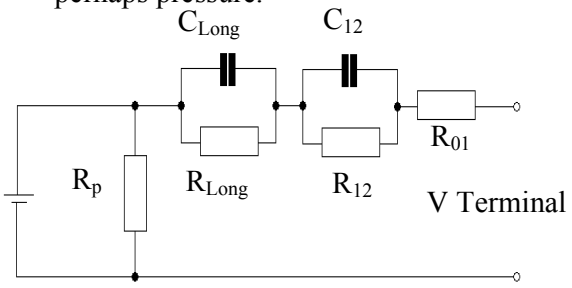

Fig. 1. Equivalent circuit model for the lithium-polymer cells during discharge.

With the exception of R_p, circuit parameters were estimated from discharge test measurements. R_{01} was obtained from: $R_{01} = |V_1\text{-}V_o|/I$ (Fig 2.). This is an instantaneous measurement, and although the equipment was set to a high sampling rate it is likely that the value of V_1 includes the beginning of the kinetic overpotential. The first second of discharge is assumed to be the instantaneous voltage drop though it is likely that, after 100ms or so, the kinetic over potential and double layer capacitance have an effect. The kinetic overpotential is affected by temperature and in turn affects the voltage (Tafel equation). The time constant is small so this should have limited effect over these scales.. In the equivalent circuit of Fig. 1, the voltage rise from V_1 to V_2 (Fig 2.) is described by a double exponential:

$$V(t) = V_1 + iR_{12}(1 - e^{-\frac{t}{R_{12}C_{12}}}) + iR_{Long}(1 - e^{-\frac{t}{R_{Long}C_{Long}}}) \quad (2)$$

These values were estimated from the data using a least squares procedure in Maple (version 9) to minimise the difference between V(t) as modelled using equation 2 and the actual data. R_{12} and C_{12} were determined from the first 300 s of the voltage rise after each pause (Fig. 2). The least squares procedure took these values and then estimated R_{long} and C_{long}. R_{12} and C_{12} found from the 15 minute pauses at the end of each 10% discharge (typically 87 mΩ and 11494 F) were significantly less than those estimated from the 2 hour pause at the end of the discharge cycle (e.g. 130 mΩ and 16026 F at 4˚C and one atmosphere). Causes for this are discussed in section 3.1. Alternative battery model options are available as given by [10], though this requires many parameters that cannot be found from the limited information available from these tests. Non-linear elements have been considered, and initial tests are encouraging. These have not been utilised here as they require high resolution tests of recovery voltage as a function of time, which has not been possible with the Digatron machine as its sampling rate is limited.

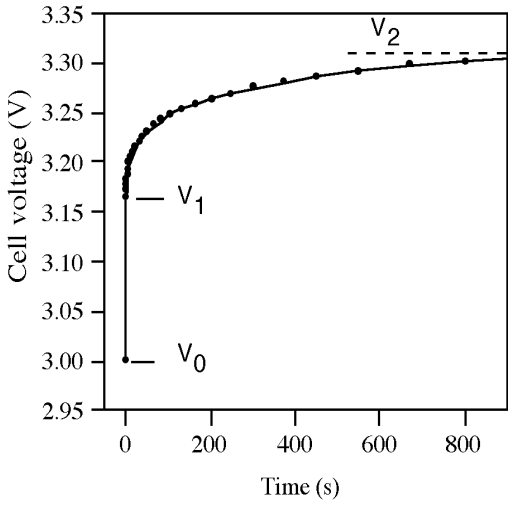

Fig. 2. Voltage-time graph of the reference cell with load of 1 A removed at T=0 showing the voltage points used to estimate the equivalent circuit parameters.

3. Analysis of Results

3.1 Electrical performance at atmospheric pressure

The cell voltage against SOC for a discharge and charge current of 1 A is shown in Fig. 3. with 15 minute pauses at intervals of $Q_0/10$. If the cell voltage reached equilibrium within each pause, then the off load voltage during discharge would be equal to the off load voltage during charge. That is not the case in these tests, for example Fig. 4 shows an enlargement graph of the data from Fig. 3. around the pause at 60% SOC.

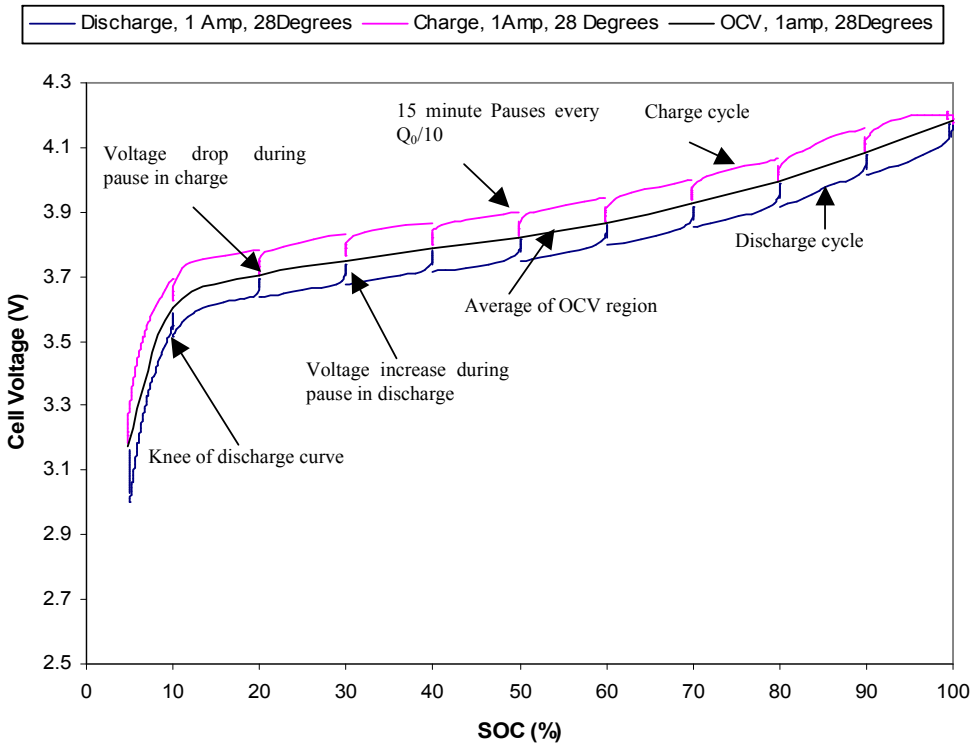

Fig. 3. Cell Voltage with state of charge during charge and discharge at 1A at a mean temperature of 28 °C at one atmosphere.

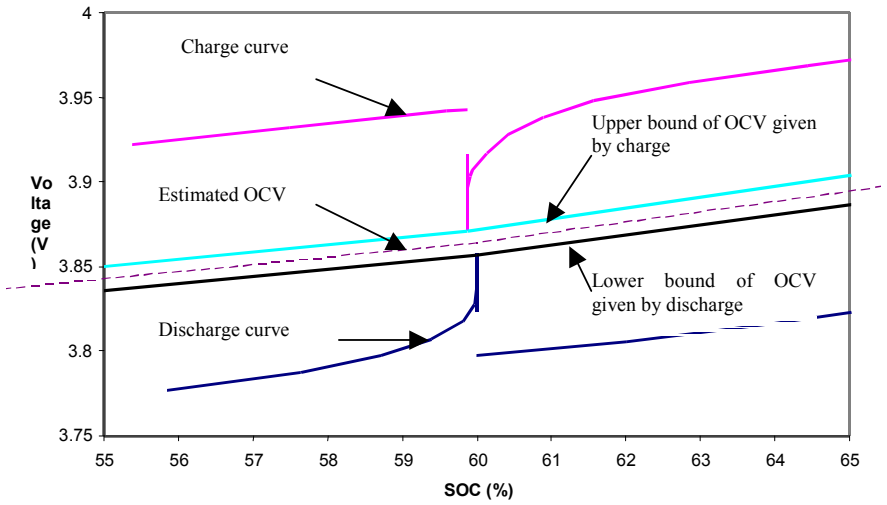

Fig. 4. Cell Voltage at 60% SOC, 1 A and mean temperature of 28 ° C showing upper and lower limits of OCV.

The gap between the cell voltages at the end of discharge and charge pauses was 14 mV. The equilibrium OCV would lie in this region. By taking the mean of the upper and lower bounds shown in Fig. 4 an estimate of the cell OCV against SOC can be made as suggested in [8], which presented experimental evidence to support this approach.

At low SOC levels, there are likely to be some electrochemical affects within the cell that will cause the OCV to be underestimated. During discharge concentration gradients of lithium ions can form at the anode or cathode, which the subsequent charging process then has to reverse. At low SOC these gradients have accumulated over the whole discharge, and so the time to offset them is increased. The end of discharge of a lithium-ion cell is determined by either reaction partners being locally depleted and/or reaction products being locally saturated, which – according to the Nernst equation - leads to a sharp decrease in the equilibrium potential of the cell. This is observed as a knee in the discharge curve and means that small changes in concentration can exhibit large changes in the cell voltage. This amplifies the effect of accumulated concentration gradients at the end of discharge. Hence, the above method for determining the OCV is likely to produce underestimated OCV at low SOC. This effect also occurs at the end of charging but it is not significant here, because the charging current tapers down at the end of charge, which would reduce the concentration gradients.

Fig. 5 shows the discharge curves for tests done at 1 A at three temperatures. All battery types experience a drop in performance with decreasing temperature [11], and this also is the case with lithium polymer cells. A discharge at 1 A still provided at least 90% of cell nominal capacity at 28°C through to 4°C. Discharge at 3.27 A provided 90% nominal capacity at 22°C yet only 65% at 4°C. A discharge at 6.5 A and 23°C still produced 85% nominal capacity, yet only 17% at 3°C.

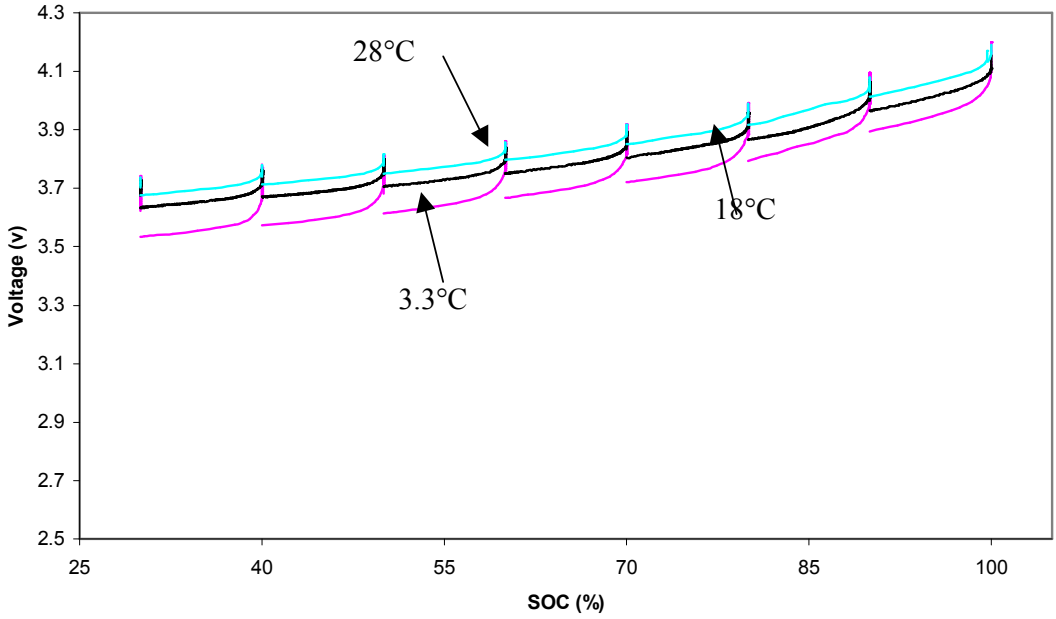

Fig. 5. Discharge curves for 1 Amp, at 28, 18, and 3.3 °C compared to SOC

After a pause the voltage rises to almost the same point at all temperatures (Fig. 5), though the estimated OCV is not quite the same. The Nernst equation in [11] shows that the equilibrium voltage is affected by a temperature coefficient, though this does not seem to be significant as the cell recovered, given 900 seconds, to the same voltage irrespective of temperature.

The drop from V_2 to the on-load voltage at the beginning of each discharge period in Fig. 7 is much larger than observed for the same current load in Fig. 6, implying an increase in R_{01} at the lower temperature. The increase of ohmic resistance (immediate voltage drop) is due to the decrease of ionic conductivity in the polymer electrolyte [12]. The increasing gradient of the discharge curve with increasing current draw is evidence of higher internal resistance R_{12} and will be explored in section 3.3. At 60% SOC, the total voltage drop at 3.27 A and 22°C is 249 mV, while at 4˚C and 3.27 A the voltage drop increases to 783mV.

The exact capacity removed from the cell is influenced by the 'knee' of the discharge curve (Fig. 3.). The cell capacity is almost fully exhausted after this knee is reached during discharge. The voltage drops quickly and only little capacity can be discharged before the cut-off voltage is reached as shown in the low current discharge in Fig 7. Fig 7 also shows that this knee is not yet reached when discharging at high currents and at a low temperature (4°C). The reason for smaller capacities obtained in these tests is not that the cell capacity is exhausted (depletion of reactants or saturation of reaction products), but that simply the cut-off voltage is reached prematurely due to high voltage drops, probably as a result of poor ionic conductivity of the polymer electrolyte.

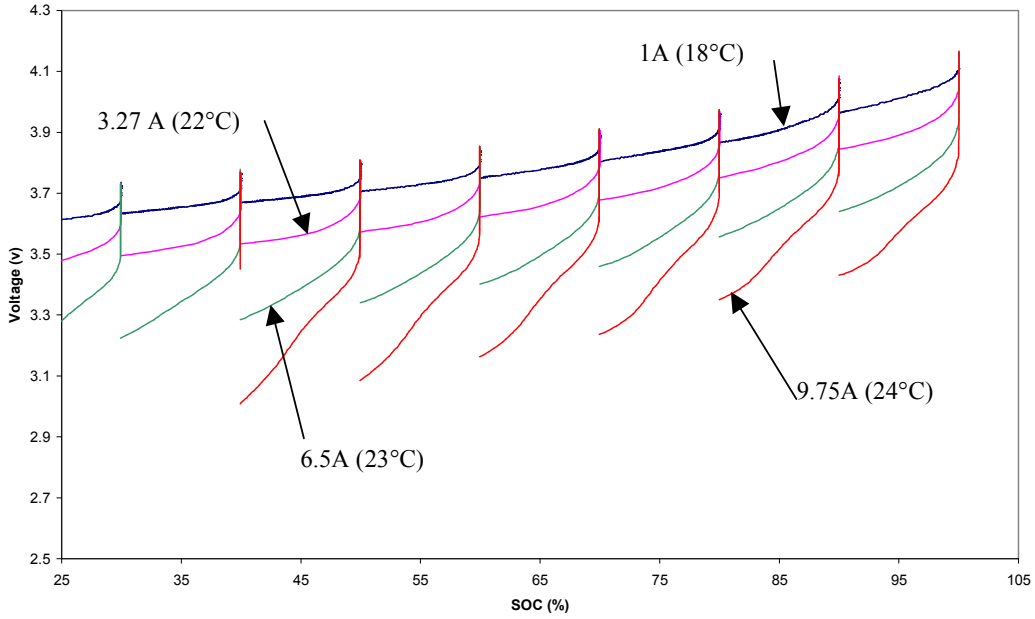

Fig. 6. Cell voltage with SOC at 1, 3.27, 6.5 and 9.75 Amp discharge between 18 and 24° C and at one atmosphere pressure.

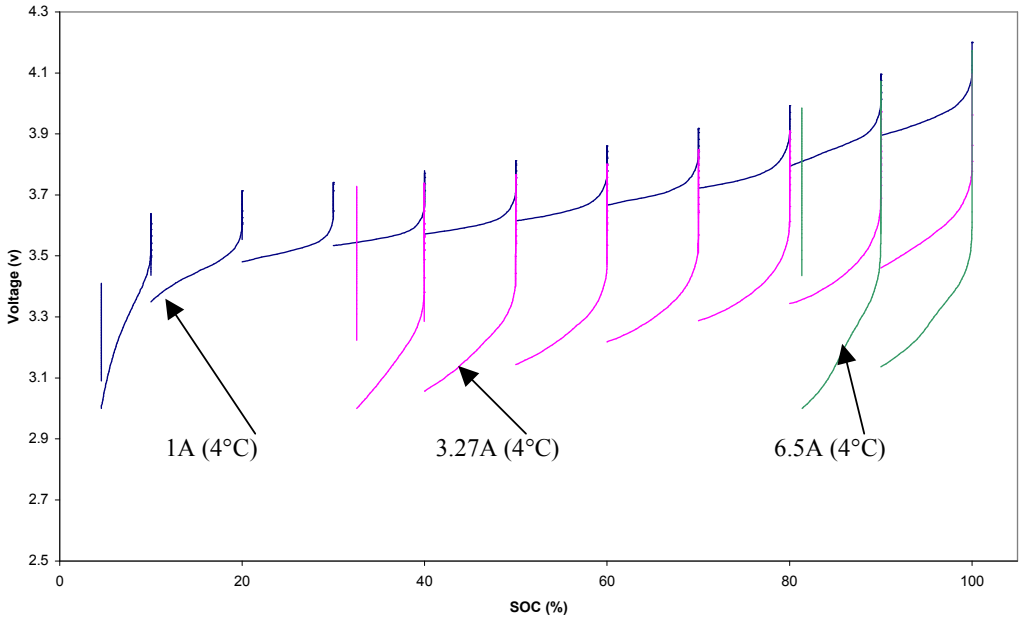

Fig. 7. Cell voltage with SOC during discharge at 1, 3.27 and 6.5 Amps, at 4° C and atmosphere pressure

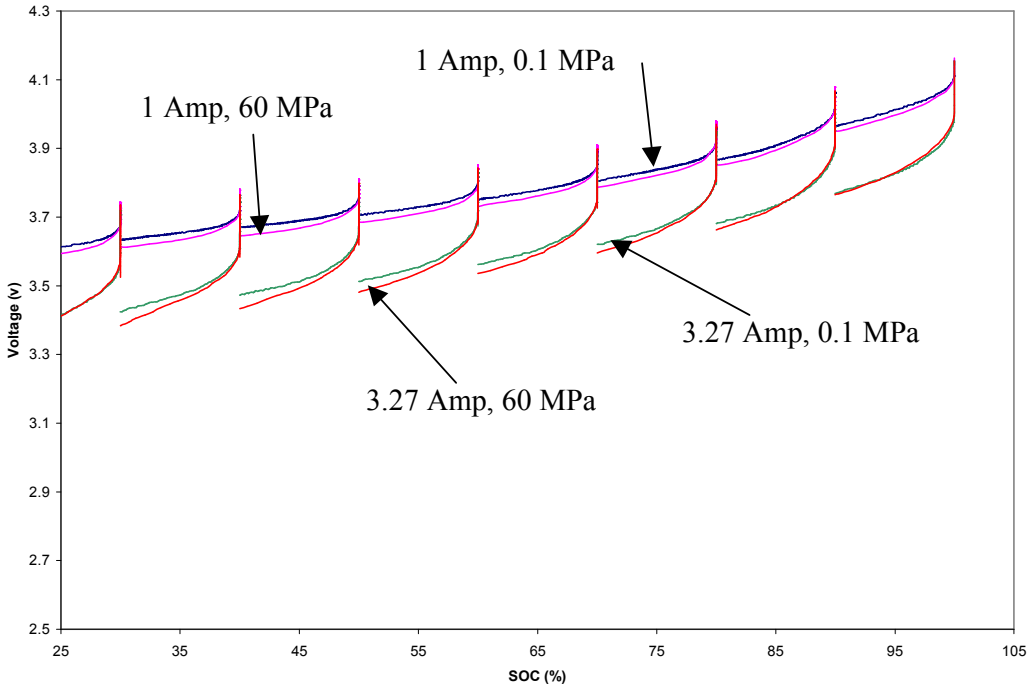

Fig. 8. Cell voltage with SOC during discharge at 1 and 3.27 A, 1 and 60 MPa at 18°C

3.2 Electrical performance at high pressure

Fig. 8 shows the voltage during discharge of tests at 1 and 3.27 A load, and at pressures of 0.1 and 60 MPa. The voltage at the end of each pause, V_2 is the same for each load at 0.1 MPa and at 60 MPa, however the discharge curve has a larger gradient when at pressure, evidence of a higher R_{12}, this will be explored in section 3.3.

Comparisons of capacity drawn from cells under 60 MPa pressure and those in atmospheric conditions have been made. At 1 A load, the capacity of the cell is 90%, slightly lower than at 60 Mpa, 91%, however an error of $\pm$ 1% is not unlikely. At 3.27 A the 60 MPa capacity is 92%, 6% higher than at 0.1 MPa, 86%, which is unlikely to be an error. This would suggest that the electrochemistry of the cell is more efficient at high pressure, though as the internal resistances are greater, this is improbable. Higher efficiency of a cell at 60 MPa would have to be repeated many times to gain confidence of this.

3.3 Equivalent circuit parameters and verification

Fig. 9 shows the estimated equivalent circuit parameters R_{01}, R_{12} and C_{12} as a function of SOC at mean temperatures of 28˚C and 4 ˚C at 0.1 MPa and at 60 MPa when discharged at 1 A. The estimated error in the calculation of the resistances is 1 mΩ and 50 F for the capacitance. The ohmic resistance R_{01} changes in both magnitude and behaviour as a function of SOC and temperature. At 28˚C R_{01} varied little with SOC, increasing from 25-26

mΩ at 100% - 30% SOC to 27-31 mΩ at 20% SOC and below. In contrast, the minimum R_{01} at 4˚C was 89 mΩ, with a rise to 164 mΩ as the cell approached 5% SOC. This ohmic voltage rise should not vary with temperature, but as discussed above in section 2.3, it is likely that this value includes a fraction of the charge transfer resistance, and so is more noticeable at 4°C.. At 60 MPa (Temperature 18˚C) the minimum R_{01} of 49 mΩ was at 90% SOC, with a rise to 71 mΩ as cell approached 5% SOC. These values are 5 – 11 mΩ larger than those found for the cell at atmospheric pressure at the same temperature.

The charge transfer resistance R_{12} behaved differently. The estimates at 0.1 MPa and 60 MPa showed higher resistances at 90% and 5% SOC than at intermediate points. At 28˚C and 0.1 MPa, R_{12} was greater than R_{01} while at 4˚C R_{12} was less than R_{01} except at 90% SOC. Also at 18˚C 60 MPa R_{12} exceeded R_{01} at 90% SOC, although not at 10% SOC and lower. Again the estimates of R_{12} at 60 MPa exceeded those at 1 bar, this time by 7-12 mΩ (except at 20% SOC where the difference of 1 mΩ is within the expected error).

Estimates of the double layer capacitance C_{12} showed lower values at the lower temperature, and highest near 50% SOC. Here tests at 18°C and 28°C have approximately the same values of C_{12}, though at pressure C_{12} could have a lower value, but still have the same curve shape.

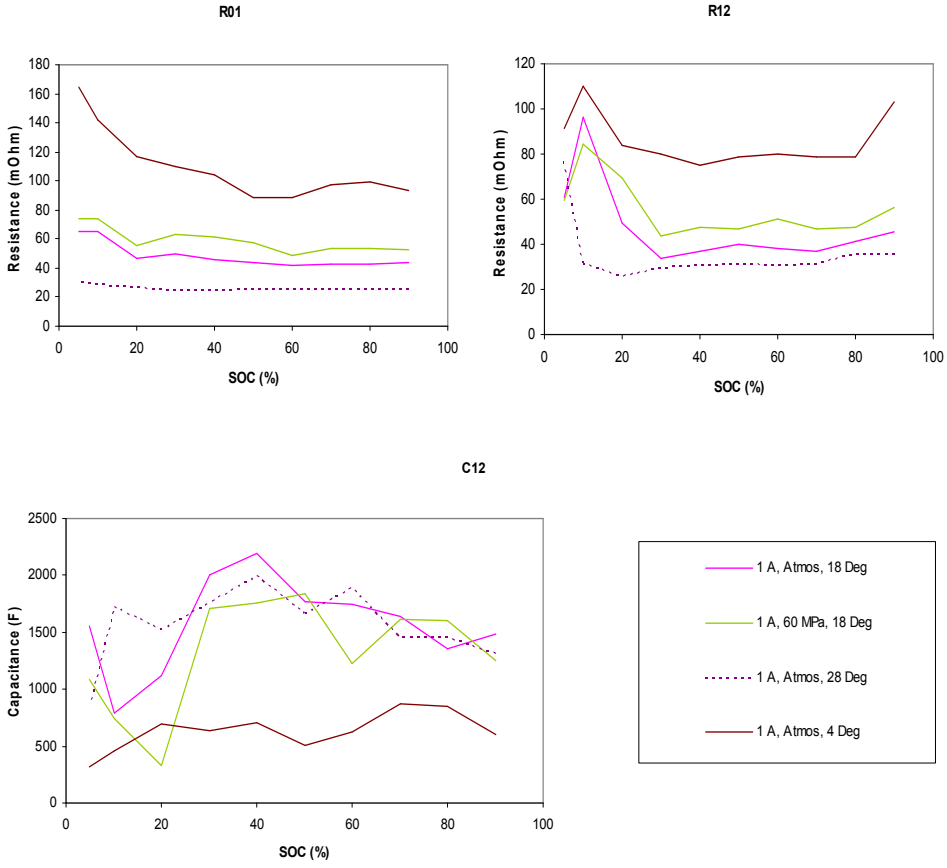

Fig. 9 Estimated Equivalent Circuit parameters R_{01} , R_{12} and C_{12} for cycles at 1 Amp and varying temperature and pressure.

The first minute of the recovery period will include the double layer capacitance, included in the Tafel equation and represented by C12, and though this value is useful for the simulating, it is not an accurate representation of the electrochemistry. The increases in resistance with pressure may also be explained by error in separating ohmic resistance and overpotentials. For the deep ocean application the cells would be far more affected by the reduction of temperature from the ocean surface to 6000 m than for the increase in pressure from 0.1 to 60 MPa. There is a small increase of resistance at pressure, but were the current draw to be kept small, the cell would still produce more than 90% of its rated capacity.

5. Conclusions

Lithium solid-polymer cells have been shown to survive repeated pressurisation to 60 MPa with no external physical failure, electrical failure, or significant degradation to on and off load voltage when returned to 0.1 MPa. This assumes isobaric conditions when these cells are housed in oil-filled pouches. As a consequence the cells have been found suitable for pressure-balanced operation within deep-diving underwater vehicles.

Cell charge capacity has been estimated as a function of temperature and current load at atmospheric pressure, and then compared to capacity at 60 MPa. There was no statistical difference in capacity at 18˚C and 1 A load (C/3) between tests at atmospheric pressure and at 60 MPa. However, at 3.27 A (1C) the capacity at 60 MPa was ~5% above that at atmospheric pressure. This increase may be the result of testing methods used, higher sampling rate tests will be needed to investigate this with more electrochemical analysis.

Analysis of charge and discharge voltage data enabled the parameters of a simple equivalent circuit model to be estimated as a function of temperature, state of charge and pressure. Temperature had a greater effect than pressure on the values of the equivalent circuit parameters. On average, the values of R_{01} and R_{12} at 60 MPa were higher, by 5-11 mΩ at atmospheric pressure at the same temperature, while cooling the cells from 18˚C to 4˚C increased R_{01} by ~60 mΩ and R_{12} by ~40 mΩ.

The equivalent circuit parameters described in this paper, will enable a model of the cell to be created, in order to then produce a fuel gauge algorithm. This algorithm would be able to predict capacity and terminal voltage based on current load, temperature and pressure. By incorporating the capacitive as well as resistive elements of the equivalent circuit within the fuel gauge algorithm the full effect could be predicted of high power pulsed loads, such as sonar transmitters or variation in AUV thrust. Improved realism in the on-board fuel gauge and battery simulator would contribute towards better utilisation and reliability of an autonomous underwater vehicle. Further work could be directed towards assessing and modelling degradation of lithium-polymer cells that have been subject to pressure cycles.

6. Acknowledgements.

The Authors would like to thank Andrew Staszkiewicz for his patience and operation of the pressure vessel.

7. References.

[1] N.W. Millard and 26 others, Multidisciplinary ocean science applications of an AUV: The Autosub science missions programme. In: Griffiths, G. (Ed.), The technology and applications of autonomous underwater vehicles. Taylor and Francis, London, 2003, pp. 139-159.

[2] P. Stevenson, G. Griffiths, A.T. Webb, The experience and limitations of using manganese alkaline primary cells in a large operational AUV. Proc. AUV 2002: A workshop on AUV energy systems, IEEE, Piscataway, 2002, pp. 27-34.

[3] G. Griffiths, G., A. Knap, T. Dickey, The Autonomous Vehicle Validation Experiment, Sea Technology, 41(2) (2000) 35-43.

[4] P. Stevenson, D. Graham, Advanced materials and their influence on the structural design of AUVs, In: Griffiths, G. (Ed.), The technology and applications of autonomous underwater vehicles, Taylor and Francis, 2003, pp. 77-92.

[5] G Griffiths, J Jamieson, S Mitchell, K Rutherford, Energy storage for long endurance AUVs. Proc. ATUV conference, IMarEST, London, 16-17 March 2004. pp. 8-16.

[6] http://www.deepsea.com/seabatry.html#summary accessed on 29 September 2004.

[7] http://www.kokam.com/product/battery_main.html accessed on 20th July 2004.

[8] S. Abu-Sharkh, D. Doerffel, Rapid test and non-linear model characterisation of solid-state lithium-ion batteries. J. Power Sources, 130 (2004) 266-274.

[9] H.Jan Bergveld, W.S.Kruijt, P.H.L.Notten, Battery Management Systems: Design by modelling, Kluwer Academic Publishers, Dordrecht, 2002.

[10] D.Lyndon, T.B.Reddy (Eds)., Handbook of Batteries, third ed., McGraw-Hill, New York, 2002, pp. 22.18

[11] G.M.Ehrlich, in: D.Lyndon, T.B.Reddy (Eds)., Handbook of Batteries, third ed., McGraw-Hill, New York, 2002, pp. 35.26

[12] http://vtb.engr.sc.edu/ last accessed on 25/02/05

[13] J. J. Hong, Lithium secondary cell and method of fabricating the same, .US Patent No. US6,423,449, 2002.